Anisotropic microfluidics and flow monitoring with a microchannel towards soft-matter sensing

Si-Chun Zhao,[a] Cong-Long Yuan,[b] Yi-Fei Wang,[b] Pei-Zhi Sun,[b] Bing-Hui Liu,[b] Hong-Long Hu,[c] Dong Shen,[a] and Zhi-Gang Zheng[*ab]

[a.] *School of Physics, East China University of Science and Technology, Shanghai 200237, China*

[b.] *School of Materials Science and Engineering, East China University of Science and Technology, Shanghai 200237, China*

[c.] *School of Chemistry and Molecular Engineering, East China University of Science and Technology, Shanghai 200237, China*

[*.] *Correspondence: zgzheng@ecust.edu.cn*

Supplementary Content

Supplementary movies

Movie S1: The transition from initial state to middle state at a constant flow rate of 200 nl min^{-1}.

Movie S2: Complete process of flow at constant flow rate of 5000 nl min^{-1}.

Movie S3: The interference colour evolution at the flow rate of 200 nl min^{-1} and 400 nl min^{-1}.

Movie S4: An air plug between the liquid crystal and the target fluid.
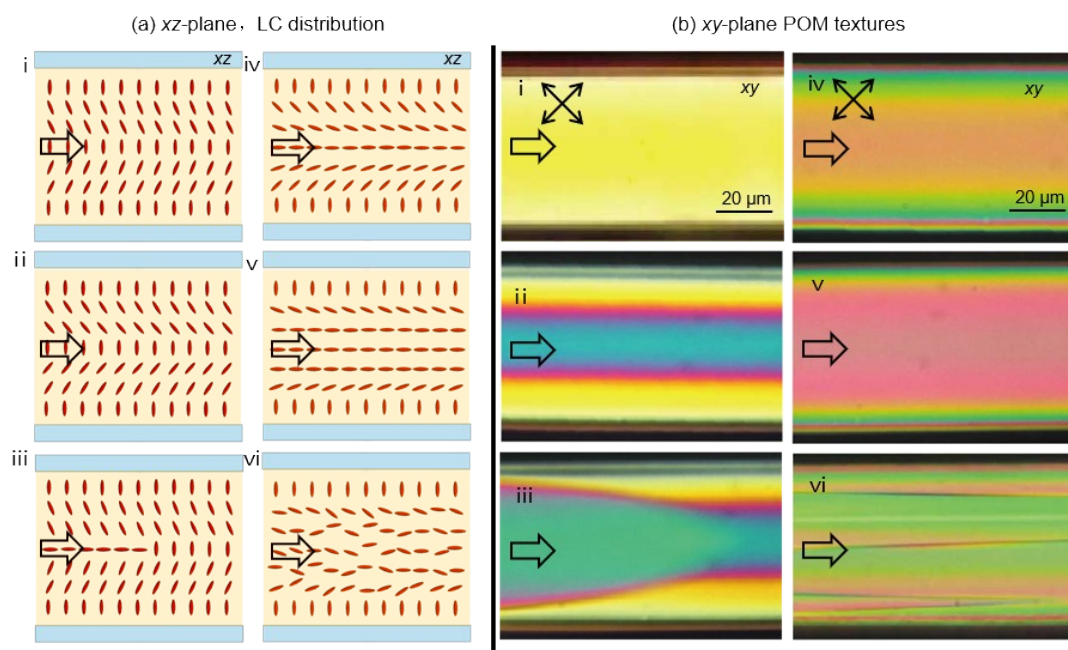
Supplementary notes and figures

Fig. S1 Evolution schematic of director field and corresponding POM texture in flow process. (a) The schematic arrangement of LC molecules in the center of the channel (*xz*-plane) along the *z* direction during the flow. The black arrow heads show the flow direction, and the blue rectangles show the upper and lower surfaces of the microchannel. (b) The image (*xy*-plane) between the crossed polarizers with the flow rate of 200 nl min^{-1}. The black arrow heads show the flow direction, with a 45° angle with the polarizers. The double arrows show the orientation of the polarizers. i Initial state, the director field is slightly deformed along the flow direction, leading to a first-order yellow between the crossed polarizers. ii Initial state, the director field undergoes further deformation and the first-order red-violet appears in the center of the channel with a rapid transition to second-order blue. iii A π/2 mutation occurred in the liquid crystal molecules at *d*/2, a parabolic transition front sweep across the channel along with discontinuous change of interference colour. iv Middle state, liquid crystal molecules at *d*/2 are aligned along the flow direction and the interference colour continue to evolve according to the order of interference colour. v Middle state, the flow-aligned regions gradually spreads upward and downward and the interference colour continue to evolve according to the order of interference colour. vi Final state, molecular arrangements are disturbed by the flow. Chaotic line defects occupy the entire channel and flow from the inlet to the outlet, and will remain throughout the final state of the flow. The scale bars are 20 μm.
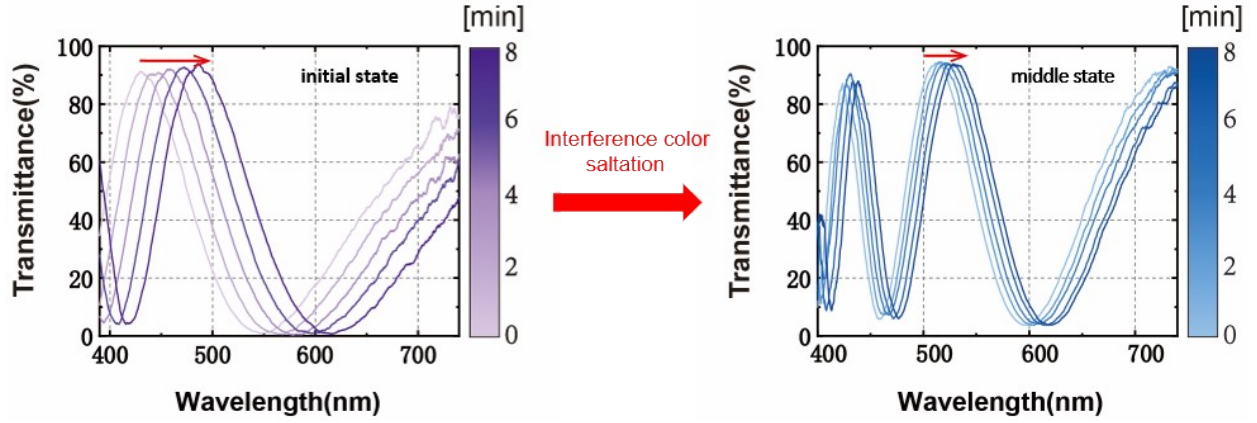
Fig. S2 The transition of the transmittance spectrum between initial state and middle state. The initial state of the spectrum redshifts faster than the middle state. In addition to saltation in spectrum positions, the spacing between peaks also changes due to the saltation in the internal director field.

The method to extend the duration time of single-pass

Flow sensing can be achieved by marking different peaks in the middle state of flow, however, due to the limitation of the spectrometer, each peak can be recorded for a limited time. We defined the time required for a particular peak to shift from 400 to 750 nm as the duration time of single-pass for that peak. This time can be used to complete one or more consecutive flow measurements, and the duration was proportional to the flow rate. In the 60×10 μm² channel, the duration time of single-pass can last 1 or 2 hours at a low flow rate and only last a few minutes at a high flow rate. Although it is still feasible to calibrate different peak values for multiple measurements in the high flow rates and will not change the sensitivity of the sensor, data discontinuity will greatly increase the difficulty and error of data processing. A viable method to avoid the error can be realized by changing the output parameters of the sensor. Herein, we propose two different physical parameters as the output of the sensor and prove their linear relationship with the flow rate.

The transmittance of the liquid crystal sample between the crossed polarizers can be written as：

$$T = \sin^2 \frac{\pi |n_{eff} - n_o| d}{\lambda_0}$$

(1)

During the flow process, the index of ordinary refraction remains constant, while the index of extraordinary refraction is related to the deflection angle θ of the LC molecule, which is an increasing function of θ ($0 \leq \theta \leq \pi/2$). Obviously, when the sample thickness remains constant, the transmittance of different bands is determined by the effective birefringence $|n_{eff} - n_o|$ of the LC sample. There is a unique effective refractive index corresponding to the LCs alignment state at any moment in the flow process. Regardless of dispersion, the effective refractive index in the direction of depth can be obtained by solving the first derivative of Eq. (1) with respect to λ:

$$n_{eff} = \frac{m\lambda_0}{d} + n_o$$

(2)

m is the number of extreme values, which is determined by how many π the phase difference changes during the

4

process of the LC molecules from being vertically aligned to being parallel to the flow direction. λ0 denotes the wavelength corresponding to the m-th extreme value. When m=1,3,5,7..., it corresponds to the 1st, 2nd, 3rd ,4th ... peaks. As defining an average polar angle $\overline{\theta}$ that describes the overall arrangement of LCs in the z dimension, the relationship between n_{eff} and $\overline{\theta}$ can be written as:
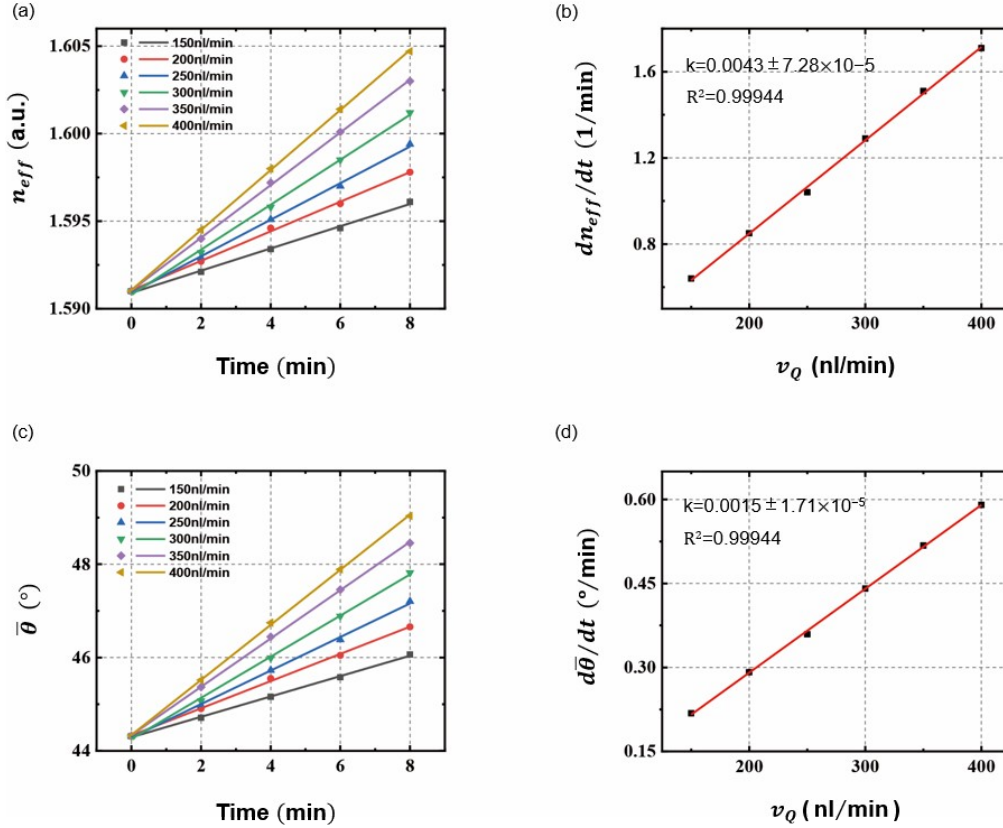

Fig. S3 (a) Variation trend of effective refractive index under different flow rate, the fitting slope of each line is the change rate of the effective refractive index at this flow rate. (b) The relationship between the effective refractive index change rate obtained by fitting and the flow rate (150 nl min⁻¹-400 nl min⁻¹). The fitting slope is the ratio of the output (effective refractive index change rate) increment to the input (flow rate) increment and represents the sensitivity of the sensor. (c) Variation trend of average polar angle under different flow rate, the fitting slope of each line is the change rate of the average polar angle at this flow rate. (d) The relationship between the average polar angle change rate obtained by fitting and the flow rate (150 nl min⁻¹ to 400 nl min⁻¹). The fitting slope is the ratio of the output (average polar angle change rate) increment to the input (flow rate) increment and represents the sensitivity of the sensor.

$$n_{eff} = \frac{n_o n_e}{\sqrt{n_e^2 \cos^2\overline{\theta} + n_o^2 \sin^2\overline{\theta}}} \tag{3}$$

Similarly, the LCs arrangement state at any moment in the flow process has a unique average polar angle corresponding to it. After converting the position information of the spectrum into the effective refractive index and the

average polar angle, the results are shown in Fig. S3. These results suggest that the sensor remains linear when the effective refractive index or the average polar angle is used as the output parameter of the sensor. By measuring the effective refractive index or average polar angle of the liquid crystal microchannel (avoiding spectral measurement), the duration time of single-pass at is no longer limited by the spectrometer, and the sensitivity of sensors is reduced in contrast.

The mechanism of liner relationship between the spectrum shift rate and the flow rate

We define the peak in the collected spectra is a function of both time and flow rate, which are expressed as:

$$\lambda = f\left(v_Q, t\right) \tag{4}$$

According to the interference peak and the birefringence anisotropy of LCs following $\Delta nd = (m + 1/2)\lambda$ and $\Delta n = n_{eff} - n_o$, the evolution of λ is regarded as the partial derivative of λ with respect to time, which can be written as:

$$\frac{\partial \lambda}{\partial t} = \frac{d}{m}\left(\frac{\partial n_{eff}}{\partial t} - n_o\right) \tag{5}$$
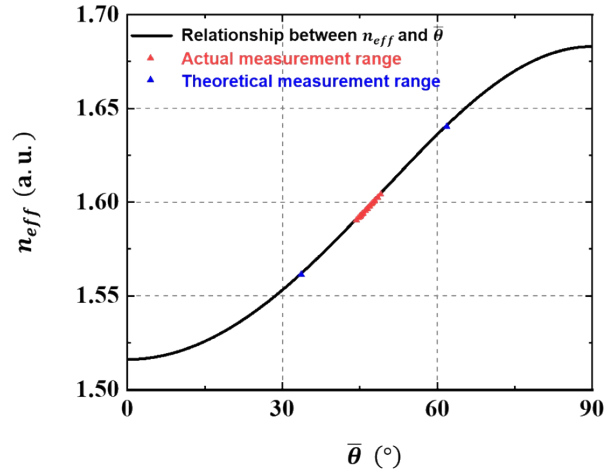

Fig. S4 The relationship between n_{eff} and $\bar{\theta}$

Figure S4 shows the relationship between the average polar angle $\bar{\theta}$ and the effective refractive index n_{eff}, where the red points are all the data points involved in the paper, and the two blue points are the data corresponding to the beginning and the end of the interference color evolution respectively. It can be clearly observed that within the measurement range the effective refractive index n_{eff} approximately shows a linear relation to the average polar angle $\bar{\theta}$. Consequently, Eq. 3 can be simplified into a linear function expressed as

$$n_{eff} = k_1\bar{\theta} + b_1 \tag{6}$$

Where k_1 and b_1 are fitting coefficients. As substituting Eq. 6 into Eq. 5, the evolution of λ can be rewritten as:

$$\frac{\partial \lambda}{\partial t} = \frac{k_1 d \partial \overline{\theta}}{m \ \partial t} + \frac{d(b_1 - n_o)}{m} \tag{7}$$

Since we have experimentally demonstrated that the change rate of $\overline{\theta}$ is linearly correlated to the flow rate v_Q in Fig. S3c-d which are expressed as:

$$\frac{\partial \overline{\theta}}{\partial t} = k_2 v_Q + b_2 \tag{8}$$

Where k_2 and b_2 are corresponding coefficients. Therefore, as substituting Eq. 8 into Eq. 7, the evolution of λ is as a linear function of the flow rate v_Q following

$$\frac{\partial \lambda}{\partial t} = \frac{k_1 k_2 d}{m} v_Q + \frac{d(k_1 b_2 + b_1 - n_o)}{m} \tag{9}$$

So that the linear relationship between the evolution rate of the interference colour and the flow rate can be theoretically interpreted.